

Using a Small Molecule Inhibitor of Peptide:*N*-Glycanase to Probe Its Role in Glycoprotein Turnover

Shahram Misaghi,¹ Michael E. Pacold,¹ Daniël Blom, Hidde L. Ploegh,* and Gregory Alan Korbel
Department of Pathology
Harvard Medical School
77 Avenue Louis Pasteur
Boston, Massachusetts 02115

Summary

Peptide:*N*-glycanase (PNGase) is ostensibly the sole enzyme responsible for deglycosylation of unfolded *N*-linked glycoproteins dislocated from the ER to the cytosol. Here we show the pan-caspase inhibitor, Z-VAD-fmk, to be an active site-directed irreversible inhibitor of yeast and mammalian PNGase at concentrations below those used to inhibit caspases *in vivo*. Through chemical synthesis we determined that the P₁ residue, electrophile position, and leaving group are important structural parameters for PNGase inhibition. We show that Z-VAD-fmk inhibits PNGase in living cells and that degradation of class I MHC heavy chains and TCR α , in an identical cellular setting, is markedly different. Remarkably, proteasome-mediated turnover of class I MHC heavy chains proceeds even when PNGase is completely inhibited, suggesting that the function of PNGase may be to facilitate more efficient proteasomal proteolysis of *N*-linked glycoproteins through glycan removal.

Introduction

Glycoproteins modulate a myriad of cellular functions such as cell-cell interactions, receptor recognition, antigenicity, and trafficking. Protein *N*-glycosylation occurs within the endoplasmic reticulum (ER), where newly synthesized glycoproteins are properly folded with the aid of ER chaperones that include calnexin, calreticulin, and BiP [1–3]. In the ER lumen, oligosaccharyl transferase cotranslationally appends a tetradecasaccharide (GlcNAc₂Man₉Glc₃) to the asparagine residue of an Asn-X_{aa}-Ser/Thr consensus sequence [4]. The lectins calnexin and calreticulin recognize the *N*-linked glycan moiety of the glycoproteins, associate with them, and mediate their ER retention until properly folded [2, 5]. Misfolded glycoproteins are extracted from the ER, ubiquitinated, deglycosylated, and subsequently degraded by cytosolic proteasomes.

Peptide:*N*-glycanase (PNGase) deglycosylates *N*-linked glycoproteins in the cytoplasm [6, 7]. PNGase cleaves the β -aspartyl-glucosamine bond between an asparagine residue and the GlcNAc residue at the reducing end of the glycan moiety, releasing a free glycan with concomitant conversion of asparagine to aspartate [8]. PNGase has been identified in, and cloned from, higher

eukaryotes [9]. The PNG1 gene product of *Saccharomyces cerevisiae* (YPng1) and its murine counterpart (MPng1) deglycosylate not only a fetuin-derived asialoglycopeptide *in vitro* [9, 10] but also deglycosylate full-length, denatured T cell receptor α chain (TCR α), CD3 δ , class I major histocompatibility complex (MHC) heavy chains (HCs) [11], and others. YPng1 prefers high-mannose oligosaccharides over complex-type oligosaccharides [11] and can discriminate between properly folded and nonnative forms of α_1 -antitrypsin null Hong Kong variant (α_1 -AT) and RNaseB [7].

Class I MHC molecules present antigenic peptides (8–10 residues), some of which are derived from intracellular pathogens, to cytotoxic T cells, thus activating defense mechanisms that ultimately result in destruction of the infected cells [12]. Through different mechanisms, the US2 and US11 gene products of human cytomegalovirus (HCMV) disrupt this process. US2 and US11 bind glycosylated class I MHC HCs and catalyze their dislocation from the ER to the cytoplasm [13, 14], where they are degraded by proteasomes. Once in the cytosol, an *N*-glycanase catalyzes the removal of the single *N*-linked glycan of class I HCs and converts the asparagine residue to an aspartate [15, 16]. Based on small interfering (si) RNA experiments, mammalian PNGase is likely the sole protein responsible for deglycosylation of class I HCs following US2-mediated dislocation from the ER [6].

Through a screen for small molecule inhibitors of YPng1, we have identified carbobenzyloxy-Val-Ala-Asp- α -fluoromethylketone (Z-VAD-fmk), a widely used broad-spectrum caspase inhibitor [17], as a potent inhibitor of yeast and mammalian PNGase. This inhibition is irreversible and likely occurs by covalent modification of the PNGase active site cysteine. We have evaluated a variety of peptidyl-fluoromethylketones as potential inhibitors of PNGase in order to probe the mechanism of inactivation. We have also analyzed the effects of Z-VAD-fmk on US2- and US11-mediated degradation of class I HCs and observed that deglycosylation occurs in the cytosol and that dislocation, deglycosylation, and proteasomal degradation are temporally distinct. We also find that inhibition of deglycosylation by Z-VAD-fmk does not impede proteasomal proteolysis of class I HCs, suggesting that glycan removal may not be a prerequisite for degradation by proteasomes. In contrast to class I HCs in US2- or US11-expressing cells, the deglycosylation and degradation of TCR α is not sensitive to the presence of Z-VAD-fmk, although degradation of TCR α is compromised by proteasomal inhibition.

Results

High-Throughput Assays Identify Z-VAD-fmk as an Inhibitor of YPng1

Fluorescence polarization and ELISA-based high-throughput assays (Figure 1A) were designed to identify inhibitors of recombinant YPng1. In the fluorescence polarization assay, fluorescein-conjugated RNaseB was used

*Correspondence: hidde_ploegh@hms.harvard.edu

¹These authors contributed equally to this work.

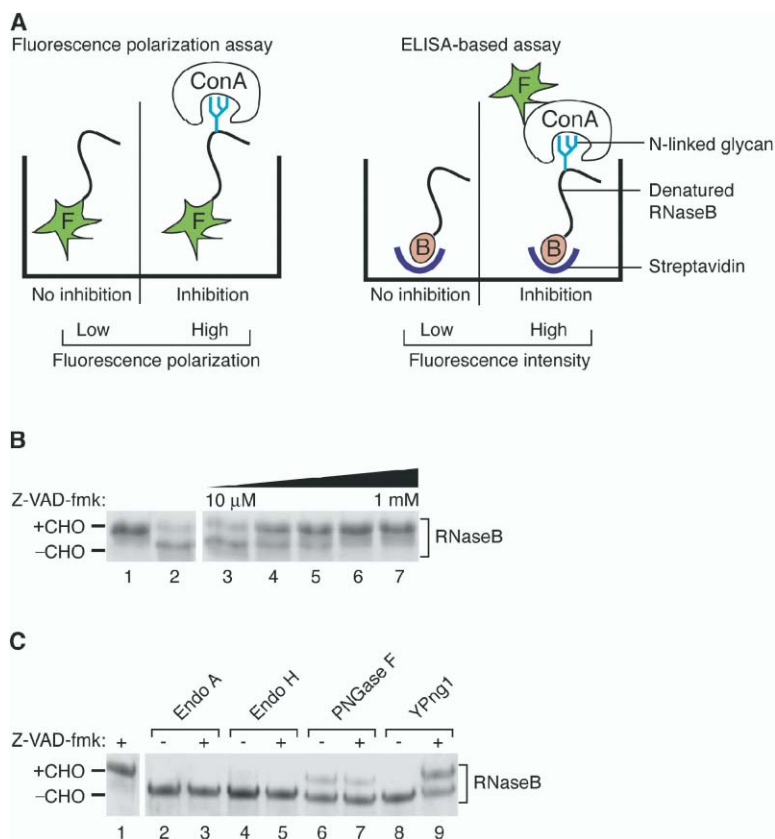


Figure 1. High-Throughput Assays Identify Z-VAD-fmk as a Potent Inhibitor of YPng1

(A) Schematic overview of the high-throughput assays. Left panel: fluorescence polarization assay in which inhibition of YPng1 results in binding of the N-linked glycan by ConA and a concomitant increase in fluorescence polarization of RNaseB-fluorescein. Right panel: ELISA-based assay in which inhibition of YPng1 leads to binding of biotinylated RNaseB by fluorescein-conjugated ConA and an increase in measured fluorescence intensity. F, fluorophore; ConA, concanavalin A; B, biotin.

(B) Z-VAD-fmk inhibits deglycosylation of denatured RNaseB by YPng1. Lane 1 contains no YPng1, while lanes 2–7 contain YPng1 (52 nM). Increasing concentrations of Z-VAD-fmk are as follows: lane 2, no Z-VAD-fmk; lane 3, 11.7 μM; lane 4, 60 μM; lane 5, 117 μM; lane 6, 600 μM; and lane 7, 1.2 mM.

(C) Z-VAD-fmk inhibits YPng1 and not other glycosidases. Endo A, Endo H, PNGase F, and YPng1 (at 3 U/reaction) were incubated for 90 min at room temperature with denatured RNaseB in the presence or absence of 100 μM Z-VAD-fmk (IC_{50} for 3 U of YPng1). +CHO and -CHO indicate the presence or absence of complete N-linked glycan, respectively.

as a substrate for YPng1. In the absence of inhibition, RNaseB is deglycosylated by YPng1, thus preventing binding of RNaseB by the lectin Concanavalin A (ConA). When YPng1 is inhibited, RNaseB retains its glycan, permitting binding by ConA and causing an increase in fluorescence polarization. In the ELISA-based assay, biotinylated RNaseB was incubated with YPng1 in the presence of potential inhibitors. The mixture was transferred to streptavidin-coated multiwell plates where the glycosylation status of RNaseB was probed with fluorophore-conjugated ConA. When YPng1 is inhibited, greater fluorescence intensity is measured.

After screening more than 100,000 compounds, we identified Z-VAD-fmk as a potent *in vitro* inhibitor of YPng1. An *in vitro* IC_{50} of 50 μM was observed for Z-VAD-fmk inhibition of RNaseB deglycosylation when YPng1 was used at a concentration of 52 nM (Figure 1B; data not shown). Z-VAD-fmk does not inhibit other endoglycosidases such as Endo A, Endo H, or the flavobacterial N-glycanase, PNGase F (Figure 1C).

Z-VAD-fmk Likely Binds Covalently to the Active Site of Yeast and Mammalian PNGase

To determine whether Z-VAD-fmk is indeed a covalent inhibitor of YPng1, we incubated the N-glycanase with Z-VAD-fmk, dialyzed the mixture to remove unreacted inhibitor, and performed matrix-assisted laser desorption/ionization mass spectrometry (MALDI-MS). We observed an *m/z* value of 43,208 daltons (Da) for YPng1 and an *m/z* value of 43,613 Da for YPng1 that had been treated with Z-VAD-fmk, a mass increase that is consis-

tent with the reaction of one molecule of Z-VAD-fmk with one molecule of YPng1 (data not shown). Additionally, dialysis failed to restore activity to YPng1 that had been treated with Z-VAD-fmk (Figure 2A, compare lanes 2 and 4). In contrast, untreated YPng1 readily deglycosylated RNaseB before and after dialysis (Figure 2A, lanes 1 and 3). To probe the site of covalent modification, we expressed a catalytically inactive mutant version of YPng1, in which the putative catalytic cysteine residue had been mutated to alanine [18]. When this C191A mutant was incubated with Z-VAD-fmk, no mass increase was observed by MALDI-MS (data not shown). When biotin-VAD-fmk was incubated with either wild-type or C191A versions of YPng1, a slight decrease in electrophoretic mobility of wild-type YPng1 compared to the C191A mutant was observed, indicating that biotin-VAD-fmk reacts only with wild-type YPng1 (Figure 2B, upper panel). This conclusion is further supported by immunoblot using a streptavidin-horseradish peroxidase (HRP) fusion protein to detect the biotinylated Z-VAD-fmk (Figure 2B, lower panel). These results suggest that binding and irreversible inactivation of YPng1 are directed at the active site and are not due to non-specific alkylation.

Next, we examined the ability of Z-VAD-fmk to inhibit the mammalian Png1. Hemagglutinin-tagged (HA) versions of both wild-type and a catalytically inactive C306A mutant [11] of murine Png1 (MPng1) were expressed in U373 astrocytoma cells, and lysates of these cells were probed with biotin-VAD-fmk (Figure 2C). Immunoblots with an anti-HA antibody (Figure 2C, upper

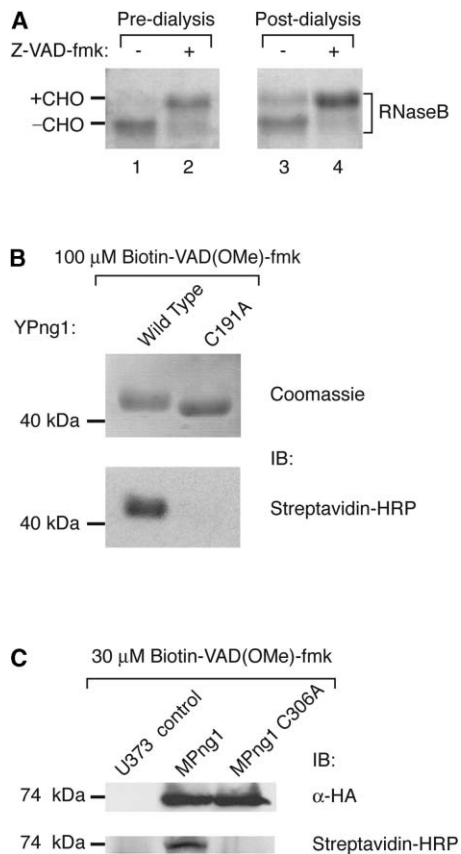


Figure 2. Z-VAD-fmk Likely Binds Covalently to the Active Site Cysteine of Both YPng1 and MPng1

(A) YPng1 (500 nM), treated with or without 100 μ M Z-VAD-fmk, was dialyzed against 1 \times NP-40 buffer containing 0.5 mM DTT to remove excess Z-VAD-fmk. Pre- and postdialysis samples of YPng1 were then incubated with denatured RNaseB and subjected to gel electrophoresis followed by Coomassie staining. +CHO and -CHO indicate the presence and absence of *N*-linked glycan, respectively.

(B) Both wild-type and C191A mutant versions of YPng1 (5 μ M) were incubated for 15 min with 500 μ M biotin-VAD-fmk and then subjected to SDS-PAGE followed by Coomassie staining (upper panel) and by immunoblot (IB) using streptavidin-HRP (lower panel).

(C) Lysates of U373 cells expressing HA-tagged versions of wild-type and C306A mutant MPng1 were labeled with 30 μ M biotin-VAD-fmk. Samples were subjected to gel electrophoresis and immunoblotted with anti-HA (upper panel) and streptavidin-HRP (lower panel).

panel) and streptavidin-HRP (Figure 2C, lower panel) showed that wild-type MPng1, but not the C306A mutant, is biotinylated. Z-VAD-fmk thus likely modifies both yeast and mammalian PNGase by covalent modification of the thiol functional group of the active site cysteine residue.

Z-VAD(OMe)-fmk Inhibits Human PNGase In Vivo

HCMV US2 and US11 glycoproteins dislocate class I HCs from the ER to the cytoplasm where they are ubiquitinated, deglycosylated, and subsequently degraded by proteasomes. Deglycosylated HC intermediates are stabilized in the presence of the proteasome

inhibitor carbobenzyloxy-Leu-Leu-Leu-vinyl sulfone (ZL₃VS), as observed by metabolic labeling [15, 16]. We have used RNA silencing in US2-expressing cells to show that class I HCs are substrates for the human PNGase, HPng1, but have been unable to achieve complete inhibition [6]. To test the ability of Z-VAD-fmk to inhibit HPng1 in US2-expressing U373 astrocytoma cells, we performed pulse-chase experiments in the presence of increasing concentrations of its cell-permeable methyl ester, Z-VAD(OMe)-fmk, and 100 μ M ZL₃VS (Figure 3A). In the absence of PNGase inhibitor, all HCs are deglycosylated within 30 min of chase. Z-VAD(OMe)-fmk inhibits endogenous HPng1 with an apparent IC₅₀ of 7 μ M, and inhibition is complete at an inhibitor concentration of 30 μ M (Figure 3A, lanes 9 and 10). For comparison, Z-VAD(OMe)-fmk concentrations ranging from 50 to 100 μ M are commonly used for caspase inhibition. To assess whether glycosylated HCs are substrates for proteasomal degradation, we performed pulse-chase experiments with or without Z-VAD(OMe)-fmk in the presence or absence of the proteasome inhibitor ZL₃VS in both US2- and US11-expressing astrocytoma cells (Figure 3B). When both US2- and US11-expressing cells are treated with ZL₃VS, the deglycosylated HC intermediates are stabilized, while in the absence of ZL₃VS these intermediates are degraded. It is striking that, while the presence of both ZL₃VS and Z-VAD(OMe)-fmk stabilizes glycosylated HCs (Figure 3B, lanes 7 and 8), the inclusion of Z-VAD(OMe)-fmk in the absence of ZL₃VS does not (Figure 3B, lanes 5 and 6). Rather, glycosylated HCs are degraded in a proteasome-dependent manner.

To confirm that the HCs observed in the presence of both ZL₃VS and Z-VAD(OMe)-fmk still carry their *N*-linked glycan, we subjected these samples to Endo H treatment (Figure 3C). The shift in molecular weight of class I HCs in the presence of Endo H corresponds to the removal of the *N*-linked glycan, indicating that the glycan on the HCs is indeed intact. To establish the subcellular location of the glycosylated HCs that are stabilized in the presence of both ZL₃VS and Z-VAD(OMe)-fmk, we performed a pulse-chase experiment with US2-expressing cells in the presence of ZL₃VS, with or without Z-VAD(OMe)-fmk, followed by subcellular fractionation (Figure 3D). In the absence of Z-VAD(OMe)-fmk, we observed deglycosylated HCs in the cytoplasm (Figure 3D, upper panel, lanes 13–15). In contrast, all HCs remain fully glycosylated in the presence of Z-VAD-fmk, regardless of their subcellular disposition (Figure 3D, upper panel, lanes 10–12 and 16–18). These results show that the process of dislocation is not compromised when PNGase is inhibited. The detection of glycosylated HCs in the cytosolic fractions when PNGase is inhibited shows that the dislocated class I HCs retain their glycan upon arrival in the cytosol. The presence of the glycan, however, does not protect the dislocated HCs from proteasomal proteolysis.

TCR α May Utilize Different Dislocation Machinery for Degradation

In the absence of the β chain of the T cell receptor, the TCR α is destroyed [19]. This degradation likely follows a pathway that involves dislocation from the ER to the cytosol and proteasomal proteolysis [20, 21]. To com-

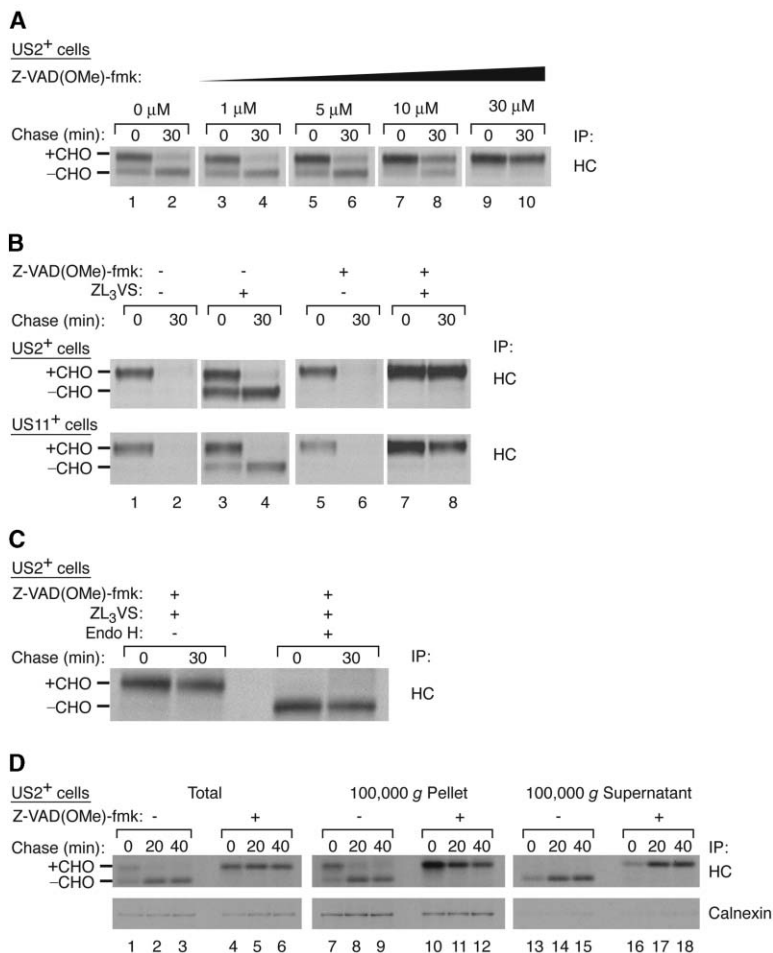


Figure 3. Z-VAD-fmk Inhibits Human PNGase Activity In Vivo

(A) Titration of Z-VAD(OMe)-fmk in US2-expressing U373 cells in the presence of 100 μM ZL₃VS as proteasome inhibitor. Cells were pretreated with the indicated inhibitors for 45 min, pulsed with ³⁵S-labeled cysteine and methionine for 15 min, and chased for the indicated periods of time in the presence of both inhibitors. Cells were lysed in 1% SDS and diluted with 1× NP-40 buffer, and class I HCs were immunoprecipitated (IP). Samples were subjected to gel electrophoresis.

(B) US2- and US11-expressing cells were pulsed/chased followed by IP of class I HCs as described in (A), in the presence or absence of 30 μM Z-VAD-fmk and 100 μM ZL₃VS as indicated.

(C) Same as described in (A), in the presence of 30 μM Z-VAD-fmk and 100 μM ZL₃VS. Samples were treated with or without Endo H prior to gel electrophoresis.

(D) Subcellular fractionation of US2-expressing cells in the presence of 100 μM ZL₃VS. Cells were pulsed/chased with or without Z-VAD(OMe)-fmk, and homogenized. One-fourth of the homogenate was used to sequentially IP class I HCs and calnexin (total fraction), and the remaining samples were spun at 100,000 × g for 1 hr. The supernatant fraction was adjusted to 0.5% NP-40, and the pellet fraction was resuspended in 1× NP-40 buffer and used for sequential IP of class I HCs and calnexin. +CHO and -CHO indicate the presence and absence of *N*-linked glycan, respectively.

pare the fate of TCR α directly with that of class I HCs, we transiently expressed TCR α in US2-expressing astrocytoma cells, where detection of deglycosylated HC molecules in the presence of proteasome inhibitor serves as an internal control for dislocation. A pulse-chase experiment was performed using untransfected US2-expressing cells or US2-expressing cells transiently expressing TCR α , in the presence or absence of proteasome inhibitor and Z-VAD(OMe)-fmk, as indicated (Figure 4A). TCR α and HC molecules were sequentially immunoprecipitated from these samples and were subjected to SDS-PAGE. As expected, deglycosylated HCs are observed in the presence of ZL₃VS, and all HCs are degraded in the absence of proteasome inhibitor (Figure 4A, lower panel, lanes 1–6, 10–12). In the presence of both ZL₃VS and Z-VAD(OMe)-fmk, glycosylated HCs are observed in the cytoplasm (Figure 3D, lanes 16–18). For TCR α expressed in the very same cells, no deglycosylated intermediates are detected, even after 3 hr of chase (Figure 4A, upper panel), a time point when the only class I HC species that persists is the deglycosylated intermediate.

If the processes of dislocation and degradation can be uncoupled for TCR α in US2/US11 cells, as we have shown for class I HCs, then it may be possible to detect deglycosylated TCR α in the cytoplasm in the presence of proteasome inhibitors. We do not observe any par-

tially or fully deglycosylated intermediates of TCR α in our pulse-chase experiments (Figure 4A, upper panel). Alternatively, if dislocation and degradation are coupled for TCR α , then addition of proteasome inhibitor may result in retention of glycosylated TCR α in the ER. To address this issue, we transiently expressed TCR α in US2-expressing cells and performed a pulse-chase experiment in the presence of ZL₃VS and the absence of Z-VAD(OMe)-fmk, and subjected the samples to subcellular fractionation followed by sequential immunoprecipitation of TCR α and class I HCs (Figure 4B). All TCR α is found in the ER fractions and is fully glycosylated (Figure 4B, upper panel, lanes 4–6). In contrast, both glycosylated and deglycosylated class I HCs are detected in the ER (Figure 4B, lower panel, lanes 4–6), and only deglycosylated HCs are observed in the cytosolic fractions (Figure 4B, lower panel, lanes 7–9). Calnexin, a control for fractionation, was found only in the pellet fraction (data not shown). These results show that the kinetics of dislocation are faster for class I HCs than for TCR α in US2- and US11-expressing cells, and further suggest that TCR α dislocation may be coupled directly to proteasomal degradation.

To show that both class I HC and TCR α molecules are substrates for glycosidases, even after treatment with ZL₃VS and Z-VAD(OMe)-fmk, we metabolically labeled these molecules and subjected them to Endo H

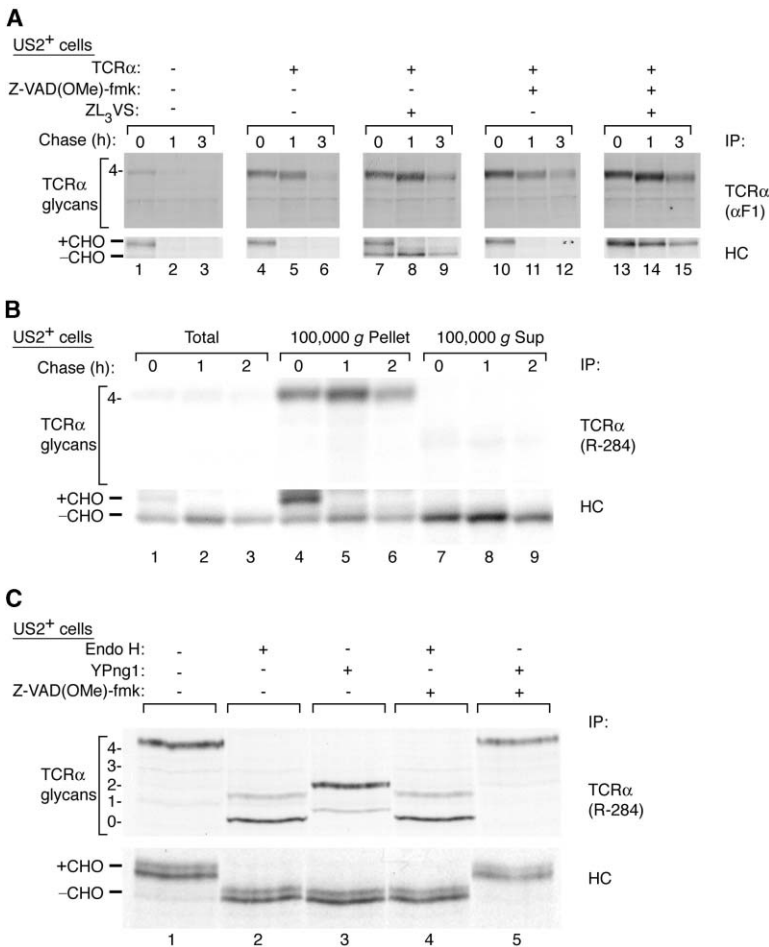


Figure 4. Dislocation and Degradation of TCRα Is Distinct from Class I HCs

(A) TCRα was transiently expressed in US2-expressing cells. Forty-eight hours posttransfection, cells were pulsed with ³⁵S-labeled cysteine and methionine for 30 min in the presence of 100 μM ZL₃VS and 30 μM Z-VAD(OMe)-fmk and chased for the indicated periods of time. Samples were lysed in 1% SDS and diluted with 1× NP-40 buffer and TCRα, and class I HCs were sequentially immunoprecipitated (IP). Untransfected US2-expressing cells were treated identically.

(B) Subcellular fractionation of TCRα yields no deglycosylated intermediates in the cytoplasm. Transient transfection and pulse-chase were performed as in (A), but without Z-VAD(OMe)-fmk. Samples were subjected to subcellular fractionation with homogenization buffer containing 2 mM *N*-ethylmaleimide, followed by sequential IP of TCRα and class I HCs.

(C) Both TCRα and class I HCs are substrates for YPng1. TCRα was transiently expressed in COS-1 cells, and 48 hr posttransfection, cells were pulsed as described in (A). Cells were lysed in 1% SDS and diluted with 1× NP-40 buffer containing 5 mM DTT. YPng1 (100 U) and Endo H (200 U) were added to the lysate in the presence or absence of 100 μM Z-VAD(OMe)-fmk, followed by overnight incubation at 4°C, followed by sequential IP of TCRα and class I HCs.

and YPng1 treatment in the presence or absence of Z-VAD(OMe)-fmk. Both Endo H and YPng1 deglycosylate fully glycosylated TCRα and HC molecules (Figure 4C, lanes 2 and 3). The presence of two prominent bands for TCRα (Figure 4C, lanes 2–4) reflects incomplete deglycosylation both by Endo H and YPng1. Z-VAD(OMe)-fmk inhibits only YPng1 (Figure 4C, lane 5) and not Endo H (Figure 4C, lane 4; see also Figure 1C, lanes 4 and 5). The subtle difference in migration of deglycosylated TCRα when treated with Endo H versus YPng1 is likely due to a single GlcNAc residue that remains at each of the four *N*-linked glycosylation sites of TCRα for the Endo H-digested sample, and the Asn → Asp conversion for the YPng1-treated sample. The doublet observed for class I HCs is most likely attributable to HLA allelic variants. The failure of YPng1 to completely deglycosylate TCRα may be due to partially folded domains and likely reflects the ability of PNGase to distinguish folded from unfolded *N*-linked glycoproteins [7]. Nonetheless, these results indicate that both class I HCs and TCRα can be deglycosylated by PNGase.

Z-VAD(OMe)-fmk Is the Most Potent Inhibitor of Human PNGase In Vivo

Fluoromethylketones constitute a class of irreversible inhibitors of thiol proteases, reacting with the active

site cysteine to yield a thioether adduct [22]. Having established that the generic caspase inhibitor, Z-VAD(OMe)-fmk, inhibits PNGase at concentrations below those commonly used to inhibit apoptosis, we explored the structural attributes that are relevant for inhibition. We evaluated a collection of related compounds for in vitro inhibition of RNaseB deglycosylation by YPng1 and for in vivo interference of HC deglycosylation in the US2/US11 system (Figure 5). The use of the free carboxylic acid versus the methyl ester of the aspartyl side chain did not affect enzymatic inhibition in vitro (data not shown). As the aspartyl residue in commercial Z-VAD(OMe)-fmk is racemic, we synthesized homochiral Z-VAD(OMe)-fmk diastereomers consisting of either D- or L-Asp(OMe)-fmk, grafted onto a Z-L-Val-L-Ala scaffold to assess the stereochemical preference of PNGase. These two diastereomers exhibited indistinguishable inhibition of YPng1 activity in vitro (Figure 6B, compare lanes 4 and 5) and of HPng1 in vivo (Figure 6C, compare lanes 5–8 and 9–12).

The proposed mechanisms of cysteine protease inactivation by fmk derivatives proceed either by direct displacement of fluoride or by initial addition of the thiolate nucleophile to the ketone carbonyl followed by sulfur migration, in both cases resulting in a thioether adduct. To address the mechanistic preference of PNGase, we synthesized homochiral diastereomers of

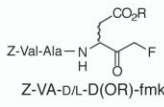
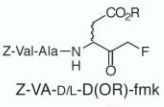
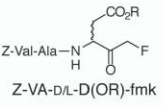
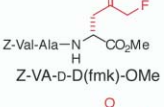
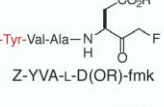
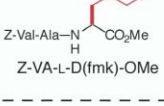
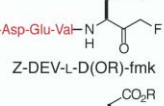
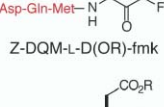
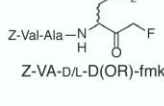
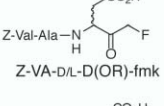
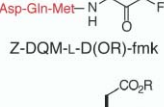
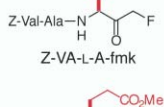
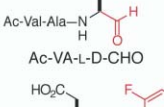
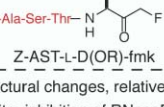
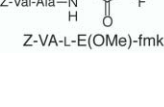
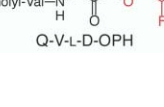
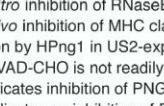
Stereochemistry			Electrophile Position			Sequence		
	<i>in vitro</i> ¹	<i>in vivo</i> ²		<i>in vitro</i> ¹	<i>in vivo</i> ²		<i>in vitro</i> ¹	<i>in vivo</i> ²
	+	+		+	+		+	+
Z-Val-Ala-D-D(OMe)-fmk	+	+		-	-		+	-
Z-Val-Ala-L-D(OMe)-fmk	+	+		-	-		+	-
Side Chain			Electrophile					
	+	+		+	+		+	-
	-	N/A		weak	- ³		+	-
	-	N/A		-	N/A		+	-
						Structural changes, relative to Z-VAD-fmk, are in red. ¹ <i>in vitro</i> inhibition of RNaseB deglycosylation by YPng1. ² <i>in vivo</i> inhibition of MHC class I heavy chain deglycosylation by HPng1 in US2-expressing cells. ³ Ac-VAD-CHO is not readily cell permeable + indicates inhibition of PNGase - indicates no inhibition of PNGase N/A indicates not tested <i>in vivo</i> for lack of <i>in vitro</i> inhibition		

Figure 5. Structural Perturbations of Z-VAD-fmk and Their Effects on Inhibition of Peptide:N-Glycanase

Z-VAD(fmk)-OMe, a derivative of Z-VAD-fmk in which the fmk warhead has been moved from the C terminus to the aspartyl side chain (Figure 6A). Neither of these compounds irreversibly inhibited PNGase activity *in vitro* (Figure 6B, lanes 6 and 7) nor *in vivo* (data not shown). The failure of these side chain warhead variants to inhibit PNGase activity is consistent with direct displacement of fluoride by the active site cysteine. Alternatively, the cysteine nucleophile may be constrained in its active site orientation and may be unable to reach C4' of the Asp(fmk)-OMe residue, thereby precluding either mechanism of inactivation. To address whether PNGase may exert a preference for attack at C2/C2' or C3/C3' of the aspartyl moiety, we desired an inhibitor in which the preferred site of attack was one carbon closer to C1. We therefore used the aldehyde-based inhibitor, Ac-VAD-CHO, where inhibition can only occur by attack at the C2/C2' position. Relative to Z-VAD(OMe)-fmk, the aldehyde inhibitor was less potent *in vitro*, providing ~60% inhibition at concentrations for which Z-VAD(OMe)-fmk completely abrogated PNGase activity (Figure 5). These results suggest that the number of atoms separating C1 of the Asp residue and the warhead is important for inhibition. Homochiral Z-VAX-fmk derivatives [X = L-Ala and L-Glu(OMe)] were also synthesized and evaluated for inhibition of YPng1 *in vitro*. Neither Z-VAA-fmk nor Z-VAE(OMe)-fmk inhibited YPng1 *in vitro*. Taken together, these results suggest that not only is warhead position an important factor

for fmk-based inhibitors, but also that PNGase, like the caspases, has a preference for Asp in the P₁ position in the type of inhibitor used here.

In light of the observed preference for aspartyl-based warheads, we evaluated a collection of related compounds for PNGase inhibition. Some tetrapeptidyl-fmk caspase inhibitors are more effective than Z-VAD(OMe)-fmk at inhibiting PNGase *in vitro* but are ineffective *in vivo* (Figure 5). As the rate of irreversible inactivation of caspases is in many cases limited by inhibitor binding, it is possible that the tetrapeptide aspartyl-fmk compounds have faster association and inactivation kinetics with their known enzymatic partners than with PNGase. The ability of Z-VAD-fmk to inhibit PNGase *in vivo* may therefore reflect more similar rates of inactivation between caspases and the N-glycanase. While we have observed that an aspartyl group is necessary for peptide-based inhibitors of PNGase, other factors can influence inhibition as well. For example, the second generation caspase inhibitor [23] quinolylcarboxy-valyl-aspartyl-(2,6-difluorophenoxy)-ketone (Q-VD-OPH) provided no detectable inhibition of YPng1 *in vitro* (data not shown)

Discussion

The observation that the broad-spectrum caspase inhibitor Z-VAD-fmk is also an inhibitor of PNGase is remarkable for two reasons. First, PNGase activity is

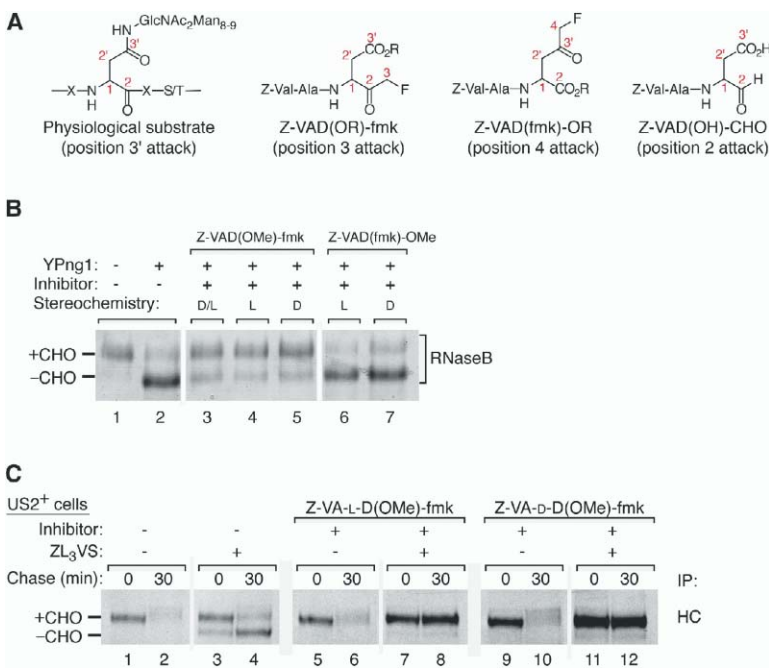


Figure 6. Electrophile Position, but Not Aspartyl Stereochemistry, Is Important for In Vitro and In Vivo Inhibition of PNGase

(A) Comparison of electrophilic inhibitors to the native substrate of PNGase. The native GlcNAc₂Man₈₋₉ substrate of PNGase and Z-VAD(OMe)-fmk have electrophiles at the C3/C3' position. Z-VAD(fmk)-OMe has an electrophile at C4, and Z-VAD-CHO has a C2 electrophile. Numbering is sequential from C_α of the aspartyl residue.

(B) RNaseB was incubated with or without YPng1 in the presence of 100 μM concentrations of inhibitors to evaluate the contributions of electrophile position and aspartyl stereochemistry on PNGase inhibition. Samples were subjected to SDS-PAGE followed by Coomassie staining.

(C) US2-expressing U373 cells were pretreated with 100 μM ZL₃VS and 30 μM Z-VAD-fmk diastereomers for 45 min, pulsed with ³⁵S-labeled cysteine and methionine for 15 min, and chased for the indicated periods of time in the presence of 100 μM ZL₃VS and 30 μM Z-VAD-fmk diastereomers. Cells were lysed in 1% SDS and diluted with 1× NP-40 buffer, and class I HCs were immunoprecipitated (IP). Samples were subjected to gel electrophoresis. +CHO and -CHO indicate the presence and absence of *N*-linked glycan, respectively.

completely inhibited by Z-VAD-fmk in living cells at concentrations that are below those commonly used to effectively inhibit caspases (Figure 3A; data not shown). This raises the interesting question whether some of the effects attributed to caspase inhibition by Z-VAD-fmk, particularly during ER-stress events and proteasomal inhibition, might be entirely or in part attributable to inhibition of PNGase. The more family-specific tetra- and pentapeptidyl fluoromethylketone caspase inhibitors and the second-generation inhibitor, Q-VD-OPH, can avert these issues in cell-based studies, since they do not inhibit PNGase in vivo (data not shown). The second remarkable aspect of Z-VAD-fmk as a PNGase inhibitor is its structure: it lacks carbohydrate modification; it contains Asp instead of Asn at the P₁ position; and it does not possess any P' residues to match the X_{aa}-Ser/Thr residues of the consensus sequence for *N*-linked glycosylation. In short, the inhibitor does not obviously mimic the molecular features that characterize the physiological substrates of PNGase. As such, high-throughput screening of a small molecule library greatly facilitated identification of Z-VAD-fmk as a non-intuitive inhibitor of this enzyme.

Through chemical synthesis of peptidyl fluoromethylketones, we have explored the structural elements relevant for inhibition of eukaryotic PNGases in vitro and in living cells (Figure 5). As with the caspases, an aspartate residue at the P₁ position of these inhibitors is important for inhibition of PNGase, but the stereochemistry at this position is not. Additionally, the position of the electrophilic trap is of critical importance for effective inhibition, optimally situated two carbon atoms away from C_α of the P₁ aspartate residue. The size of the leaving group may also be critical, with large leav-

ing groups not being tolerated. From these data we have arrived at a possible mechanism of PNGase inhibition by aspartyl fluoromethylketones such as Z-VAD-fmk (Figure 7). Recognition of Z-VAD-fmk by PNGase occurs through the aspartyl side chain, possibly via the side chain carbonyl. Upon binding (step 1), there is a reorganization of the active site architecture, initiating the shuttle of protons (step 2) that leads to a highly nucleophilic thiolate on the active site cysteine. Rotation of the C_α-N bond at the aspartyl residue of the inhibitor (step 3) moves the electrophilic C-F moiety in proximity of the cysteine nucleophile, and fluoride displacement (step 4) leads to irreversible inactivation by formation of a stable thioether bond.

PNGase is responsible for recognizing and removing the high-mannose sugar complexes of glycoproteins dislocated from the ER to the cytosol [11]. This deglycosylation event is proposed to precede, yet be coupled with, proteasomal degradation [11, 24]. Consistent with this idea, an association between YPng1 or MPng1 with Rad23, a protein with an N-terminal ubiquitin-like domain that can bind to proteasomes, supports a possible physical interaction between Png1 gene products and the proteasome [9]. PNGase deglycosylates unfolded glycoproteins and distinguishes these substrates from glycoproteins in their native conformation [6, 7, 11]. However, as PNGase is dispensable in yeast, the physiological importance of this enzyme in other organisms is unclear. The localization of PNGase has been suggested to be cytosolic [11, 25] or ER associated, possibly even within the ER lumen [26]. However, PNGase lacks signals known to be involved in import into the ER, cotranslationally or otherwise. Changes in the intracellular site of deglycosylation would be ex-

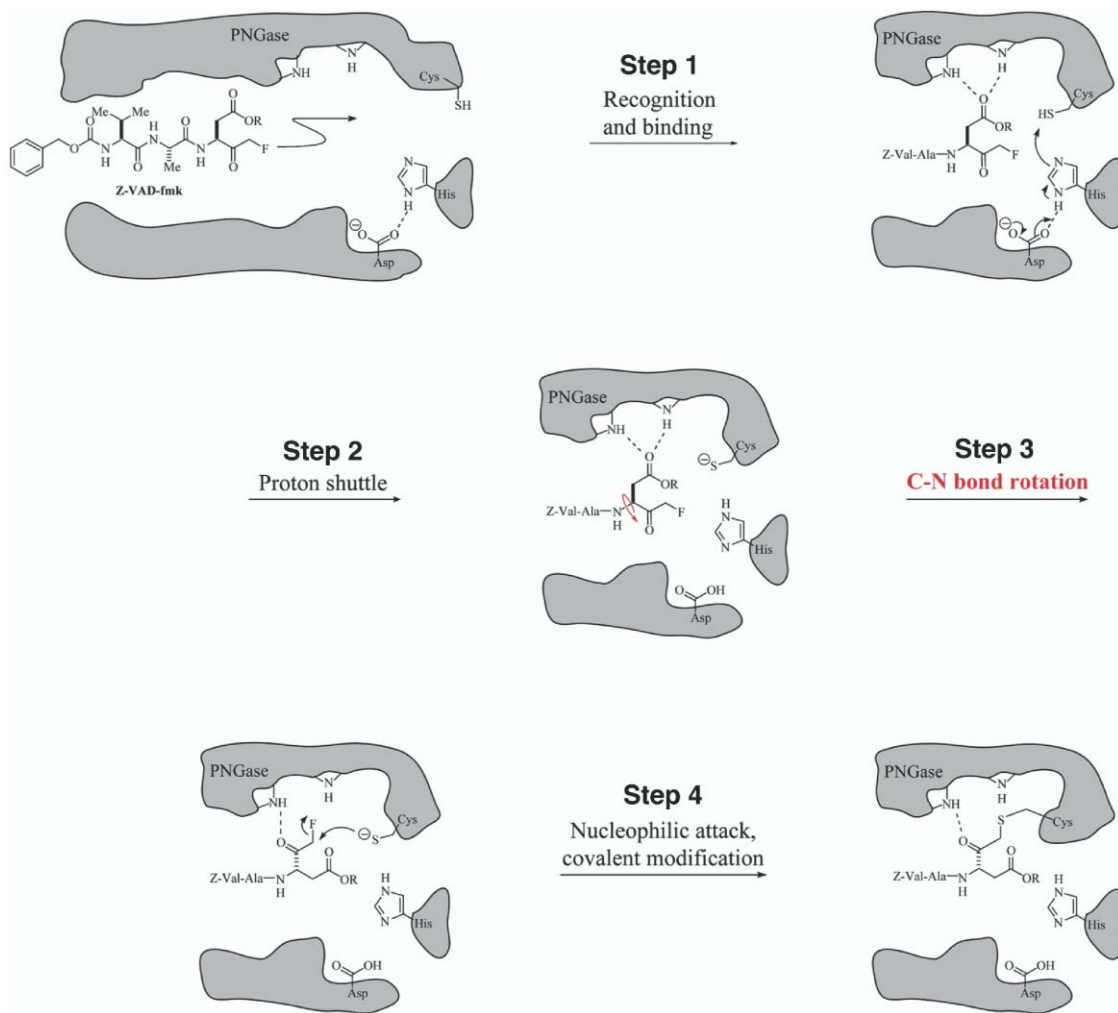


Figure 7. Proposed Mechanism of Inhibition of PNGase by Z-VAD(OMe)-fmk or Z-VAD-fmk

The inhibitor enters the *N*-glycanase active site, and binding is mediated by recognition of the aspartyl side chain. Upon binding, a conformational change in the enzyme brings together the catalytic triad (Asp, His, Cys) facilitating a shuttle of protons that leads to deprotonation of the active site cysteine thiol. In the absence of a suitable electrophile, the enzyme is stalled at this thiolate stage. Rotation of the C α -N bond at the aspartyl residue of the inhibitor positions the electrophilic carbon atom appropriately for attack by the cysteine nucleophile with concomitant displacement of a fluoride ion. The resulting thioether bond is stable and provides irreversible inactivation of PNGase.

pected to alter the timing of PNGase activity and therefore change the order of molecular events in the overall degradation pathway(s). Whether the sequence of events in the dislocation/peptidolysis pathway is the same for most or all substrates remains to be determined.

The HCMV glycoproteins US2 and US11 subvert the maturation of class I HCs by facilitating their rapid dislocation from the ER to the cytosol. US2 and US11 recognize different conformations of HCs and they utilize different machinery to extrude HCs from the ER. Based on the sensitivity to structural alterations in the class I MHC substrate [6], the sensitivity to mutations in cytoplasmic tail or transmembrane segments (P. Stern, M.J. Kim, M.E. Lorenzo, H.L.P., D. Tortorella, unpublished data), as well as the effects of dominant-negative versions of a mammalian Der1-related protein, derlin-1 [14, 27], the US2- and US11-dependent dislocation path-

ways are clearly distinct. Despite the differences between US2- and US11-mediated dislocation of class I HC, both pathways converge on common cytosolic deglycosylation and degradation events, the former of which is sensitive to inclusion of Z-VAD(OMe)-fmk (Figure 3B).

When HPng1 is inhibited by Z-VAD(OMe)-fmk, we observe intact and fully glycosylated HCs in US2- and US11-expressing cells in the presence of the proteasome inhibitor ZL₃VS (Figure 3B, lanes 5–8). Subcellular fractionation of US2-expressing cells in the presence of proteasome inhibitor indicates the presence of deglycosylated HCs associated with the membrane fraction in the absence of Z-VAD-fmk (Figure 3D, lanes 7–9). This suggests a mechanism in which HCs encounter PNGase at the ER membrane during dislocation, at which point their *N*-linked glycans are removed prior to their release into the cytosol for proteasomal proteoly-

sis. Functional HPng1 is clearly not an absolute requirement since its inhibition does not preclude dislocation or degradation of class I HCs in US2- or US11-expressing cells when proteasomes are not inhibited (Figure 3B, lanes 5 and 6). The physiological role of PNGase, therefore, may be to remove the carbohydrate moiety from *N*-linked glycoproteins in order to provide for more efficient proteasomal proteolysis.

In contrast to class I HCs, we do not detect TCR α that has exited the ER when proteasomes are inhibited (Figure 4B). Inhibition of HPng1 deglycosylating activity with Z-VAD(OMe)-fmk in the absence of proteasome inhibitor did not markedly affect degradation of fully glycosylated TCR α in US2-expressing U373 astrocytoma cells (Figure 4A), COS-1 cells, or HEK 293 cells (data not shown), nor are intermediates detected under these conditions. Detection of deglycosylated TCR α , as previously reported [21], can be accounted for by post-lysis deglycosylation, since lysis in the presence of either NEM or SDS fails to yield detectable deglycosylated TCR α .

The absence of partially or fully deglycosylated intermediates of TCR α in the pellet fraction in the absence of Z-VAD-fmk is notable and is inconsistent with a luminal ER disposition of PNGase, because deglycosylation would then be expected to proceed also on glycoprotein substrates retained in the ER. It is likewise inconsistent with the dislocation/degradation mechanism proposed for class I HCs, because significant amounts of cytosolic TCR α species are not observed even when proteasomal proteolysis is blocked.

In cells actively engaged in degradation of US2- and US11-dislocated class I HCs, the breakdown of TCR α , expressed in the very same cells, proceeds without the obvious formation of soluble intermediates sensitive to inclusion of Z-VAD-fmk or ZL₃VS. If the persistence of deglycosylated HC intermediates in the presence of ZL₃VS were attributable to stabilization and complete inhibition of proteasomal proteolysis, then TCR α should also yield such intermediates, if the mechanisms of dislocation were similar for HCs and TCR α . We therefore conclude that the overall dislocation/degradation mechanisms for these two glycoproteins are different.

Significance

Two alternative pictures emerge from our data. One possibility involves strict coupling of dislocation with deglycosylation and proteasomal proteolysis for substrates such as TCR α , and weak or no coupling of these events for the US2- and US11-mediated degradation of class I HCs. Alternatively, detection of proteins dislocated from the ER to the cytosol, glycosylated or not, may depend on the flux of extruded proteins. The rate of dislocation of class I HCs in US2- or US11-expressing cells is faster than that of class I HCs in the absence of both exogenous viral proteins or β_2m [6], and is considerably faster also than that of TCR α . The observation of cytosolic HCs may therefore be due to an inability of cytosolic proteasomes to outpace the rate of dislocation of this protein when in the presence of US2 or US11. While HPng1 may be involved in deglycosylation of *N*-linked glycoproteins

destined for degradation by proteasomes, its activity is not an absolute requirement, since HPng1 inhibition does not preclude proteolysis of class I HCs by proteasomes in US2- and US11-expressing cells. The physiological role of PNGase, therefore, may be to remove the carbohydrate moiety from *N*-linked glycoproteins in order to provide for more efficient proteasomal degradation.

Experimental Procedures

Plasmid Constructs

Histidine-tagged yeast Png1 (YPng1-His₆) was amplified using the primers described below and cloned into the NcoI and XhoI sites of the pET-28a(+) vector (Novagen): sense, CATGCCATGGGAGA GGTATACGAAAAA; antisense, CCGCTCGAGTTTACCATCTCCC CACGCTG.

Wild-type and site-directed mutant (C306A) mouse Png1 (MPng1) genes were cloned and expressed as described previously [11].

Png1 Expression and Purification

BL21/DE3 *Escherichia coli* bacteria transformed with YPng1-His₆ plasmid were grown at 37°C (30 mg/l kanamycin) and induced for 3 hr with IPTG (1 mM). Cells were harvested and lysed in buffer A (20 mM Tris [pH 8], 100 mM NaCl, 5% glycerol) containing 5 mM imidazole and 1% Triton X-100. Lysate was loaded on a Ni²⁺-NTA column (QIAGEN) equilibrated with buffer A. The column was washed with five column volumes (CV) of buffer A containing 10 mM imidazole and 0.1% Triton X-100, followed by 10 CV of buffer A containing 15 mM imidazole. Png1-His₆ was eluted with 5 CV of elution buffer (200 mM imidazole, 1 mM DTT in buffer A). The eluted Png1-His₆ was diluted 4 \times with buffer B (20 mM Tris [pH 8], 25 mM NaCl, 10% glycerol, 1 mM DTT, and 5 mM EDTA) and was loaded on a Uno-Q12 (BioRad) ion exchange column. The column was first washed with 3 CV of buffer B, and then the salt concentration was increased over 15 CV to 25% of buffer C (buffer B containing 1 M NaCl). Fractions containing YPng1-His₆ were dialyzed against buffer D (buffer B containing 150 mM NaCl) and concentrated to 4.7 mg/ml (0.11 mM).

Cell Lines, Antibodies, and Compounds

U373-MG astrocytoma cells stably expressing US2 or US11 were generated as described [6, 14]. Cells were selected and grown in Dulbecco's modified Eagle's medium (DMEM), supplemented with 5% fetal calf serum and 5% calf serum. Cells were selected using neomycin at a concentration of 0.5 mg/ml. HC70 antibody [28] recognizes free class I MHC heavy chains (HCs). The 12CA5 (Roche) antibody recognizes HA-epitopes, and the anti-calnexin monoclonal antibody was AF8 [29]. R-284 is a rabbit polyclonal antibody to TCR α [21]. α F1 is a mouse monoclonal antibody to TCR α and was a kind gift from Kai Wucherpfennig. Immunoprecipitation (IP) was performed using the following volumes of antibody per IP: HC-70 (3 μ l), R-284 (1 μ l), α F1 (1 μ l), and AF8 (1 μ l). Endo H and PNGase F activities were 500 U/ μ l (NEB). Endo A was cloned and purified from *Arthrobacter protophormiae* with activity of 480 U/ μ l [30]. Endo A, Endo H, and PNGase F were used at 3 U/reaction unless indicated otherwise. Z-VAD-fmk, Biotin-VAD(OMe)-fmk, Z-YVA-D(OMe)-fmk, Z-D(OMe)QMD(OMe)-fmk, and Z-ASTD(OMe)-fmk were obtained from Sigma (St. Louis). Z-VAD(OMe)-fmk was obtained from Promega, and Z-DEVD-cmk, Z-D(OMe)EVD(OMe)-fmk and Z-YVAD-fmk were obtained from Bachem (King of Prussia, PA). Q-VD-OPH and Z-VAD-CHO were obtained from Enzyme Systems (Livermore, CA).

Metabolic Labeling, Immunoprecipitation, and Subcellular Fractionation

Cells were metabolically labeled with 500 μ Ci of ³⁵S methionine/cysteine (NEN-Dupont), lysed in 1% SDS followed by dilution with

NP-40 buffer, and immunoprecipitated as described [31]. Subcellular fractionation of cells was performed as described [28].

High-Throughput Assays

Fluorescence Polarization Assay

Bovine pancreatic RNaseB (Sigma) was dissolved in 1 ml of 1× NP-40 (25 mM Tris [pH 7.4], 0.5% NP-40, 100 mM NaCl, and 5 mM MgCl₂) plus 6 M urea and 8 mM DTT to a final concentration of 0.6 mM and was incubated at 37°C for 30 min. 5-iodoacetamidyl-fluorescein (Molecular Probes, Eugene, OR) was added (6 mM final), and the solution was incubated for 1 hr, followed by the addition of iodoacetamide (Sigma, 100 mM final) and an additional 30 min incubation. The solution was diluted to 3 ml in 1× NP-40 buffer and dialyzed four times, each against 1 liter of 1× NP-40 plus 5 mM DTT. The RNaseB-fluorescein was diluted to 2 liters with 1× NP-40 (~100 nM final) and stored at -20°C in dark. For the assay, RNaseB-fluorescein was diluted to 25 nM in 1× NP-40 containing 5 mM DTT. A μ fill dispenser (Bio-tek, Winooski, VT) was used to dispense 20 μ l of substrate per well of black 384-well plates (Nunc, Rochester, NY). Compounds used in the screen were made available by the Institute for Chemistry and Cellular Biology (ICCB, Harvard Medical School, Boston, MA) as stock solutions in DMSO from which aliquots were transferred using a Seiko robot equipped with a 100 nl-384-pin transfer array. YPng1 was added to 10 nM final concentration (5 μ l of 50 nM solution, in 1× NP-40 plus 5 mM DTT, per well) and plates were incubated at 25°C for 3 hr. Concanavalin A (Sigma, 5 μ l of 100 μ M stock in 1× NP-40 containing 10 mM MnCl₂ and 10 mM CaCl₂) was added to each well followed by 3 hr incubation at 25°C. Plates were read in an Analyst (LJL BioSystems, Sunnyvale, CA) fitted with a 505 nm beamsplitter. Three measurements of 0.1 s, with a Z height of 2 mm from plate bottom, were collected and averaged for each well (PMT in comparator mode and emission polarizer in dynamic mode). The g factor was 1, and the plate settling time was 150 ms. Measurements were reported in counts per second, and the maximum fluorescence polarization was determined in the absence of YPng1. Baseline fluorescence intensity was determined from wells containing no transferred compounds. Data were exported as text files, converted to lists with the program FP2list, and evaluated with Spotfire (Spotfire, Inc., Somerville, MA).

ELISA-Based Assay

All hits from the fluorescence polarization assay were analyzed with an ELISA assay, which measures the amounts of glycosylated RNaseB-biotin. RNaseB-biotin was prepared in a manner similar to RNaseB-fluorescein, with the substitution of biotin iodoacetamide (Molecular Probes) for 5-iodoacetamidyl-fluorescein. Assays were set up using volumes and concentrations of substrate, inhibitor, and YPng1 identical to those used in the fluorescence polarization assay. After 3 hr at 25°C, the reactions were quenched with 25 μ l of 20 μ M NEM in H₂O. A 40 μ l aliquot was transferred to a black, 384-well, streptavidin-coated plate (Sigma) and incubated for 1 hr at 25°C, and the wells were washed four times with 80 μ l of PBS. Then 50 μ l of 2 μ g/ml Concanavalin A-fluorescein (Molecular Probes) in PBS was added to each well, incubated for 1 hr at 25°C, and washed four times with 80 μ l of PBS. The wells were filled with 50 μ l of PBS, and after 3 hr incubation at 25°C the fluorescence intensity of the wells was read with an Analyst (LJL BioSystems) fitted with a 505 nm beamsplitter. Three 0.1 s measurements were collected from a Z height of 3 mm and averaged (PMT set to comparator mode, plate settling time = 150 ms). All data were reported in counts per second.

Gel Shift Assay

The resulting small set of lead compounds that exhibited inhibition of YPng1 in the ELISA-based assay were directly analyzed by a gel shift assay. A 15 μ l aliquot of 12.2 μ M RNaseB-biotin was mixed with 1 μ l of 0.9 μ M YPng1 in 8 mM DTT and 1 μ l of inhibitor in DMSO. Reactions were run for 30 min at 25°C, quenched with 5 μ l of 4× SDS loading buffer, and run on a 15% denaturing polyacrylamide gel. The proteins were detected by Coomassie blue staining. YPng1 activity was indicated by a decrease in the molecular mass of the RNaseB, corresponding to loss of the N-linked glycan.

In Vitro and In Vivo Deglycosylation Assays

For in vitro assays denatured RNaseB was used at 0.2 mg/ml (12 μ M) and YPng1 was used at 52 nM final concentration. The reac-

tions were carried on in 1× NP-40 buffer containing 0.5 mM DTT for 30 min at 25°C. Specified inhibitors were added as indicated for each experiment, and an equal amount of DMSO was added to all controls. In vivo assays were performed using US2- or US11-expressing cells. Cells were incubated for 45 min with the indicated inhibitors in starvation media prior to the pulse. Cells were pulsed with ³⁵S methionine/cysteine and chased with an excess of nonradiolabeled methionine/cysteine for the indicated time periods. Samples were then subjected to SDS-PAGE. DMSO was added to all the controls.

Mass Spectrometric Analysis

YPng1 (5 μ M) was incubated with or without 20 μ M Z-VAD-fmk in 1× NP-40 buffer containing 0.5 mM DTT (200 μ l total volume) for 1 hr at room temperature then dialyzed against 200 ml of 25% acetonitrile and 0.5% trifluoroacetic acid in water and analyzed by matrix-assisted laser desorption ionization mass spectrometry (MALDI-MS). An analogous procedure was performed for the C191A mutant YPng1.

Synthesis of Fluoromethylketone Derivatives

When appropriate, Boc-protected amino acids were prepared as reported [32]. General syntheses, including the preparation of monobenzyl fluoromalonic acid magnesium salt, were based on the methods reported previously [33]. Pure products were obtained as white solids by recrystallization from isopropanol/hexanes.

Supplemental Data

Supplemental data, consisting of physical characterization of compounds, including NMR data, are available at <http://www.chembiol.com/cgi/content/full/11/12/1677/DC1/>.

Acknowledgments

We thank Brian DeDecker, Steve DeWall, and the ICCB facility at Harvard Medical School for their advice and assistance with high-throughput assays, Shaw Huang of the Harvard Chemistry Department for access to instruments for ¹⁹F-NMR acquisition, and Eric Spooner of the Pathology Functional Proteomics Core facility at Harvard Medical School for mass spectrometric analysis. We also thank Christian Hirsch for technical help and Howard Hang for insightful discussions. M.P. was supported by a Paul and Daisy Soros Fellowship.

Received: September 24, 2004

Accepted: October 1, 2004

Published: December 17, 2004

References

1. Ellgaard, L., Molinari, M., and Helenius, A. (1999). Setting the standards: quality control in the secretory pathway. *Science* 286, 1882–1888.
2. Ellgaard, L., and Helenius, A. (2001). ER quality control: towards an understanding at the molecular level. *Curr. Opin. Cell Biol.* 13, 431–437.
3. Ellgaard, L., and Helenius, A. (2003). Quality control in the endoplasmic reticulum. *Nat. Rev. Mol. Cell Biol.* 4, 181–191.
4. Dempski, R.E., Jr., and Imperiali, B. (2002). Oligosaccharyl transferase: gatekeeper to the secretory pathway. *Curr. Opin. Chem. Biol.* 6, 844–850.
5. Wearsch, P.A., Jakob, C.A., Vallin, A., Dwek, R.A., Rudd, P.M., and Cresswell, P. (2004). Major histocompatibility complex class I molecules expressed with monoglucosylated N-linked glycans bind calreticulin independently of their assembly status. *J. Biol. Chem.* 279, 25112–25121.
6. Blom, D., Hirsch, C., Stern, P., Tortorella, D., and Ploegh, H.L. (2004). A glycosylated type I membrane protein becomes cytosolic when peptide: N-glycanase is compromised. *EMBO J.* 23, 650–658.
7. Hirsch, C., Misaghi, S., Blom, D., Pacold, M.E., and Ploegh, H.

- H.L. (2004). Yeast N-glycanase distinguishes between native and non-native glycoproteins. *EMBO Rep.* 5, 201–206.
8. Plummer, T.H., Jr., Elder, J.H., Alexander, S., Phelan, A.W., and Tarentino, A.L. (1984). Demonstration of peptide:N-glycosidase F activity in endo-beta-N-acetylglucosaminidase F preparations. *J. Biol. Chem.* 259, 10700–10704.
 9. Park, H., Suzuki, T., and Lennarz, W.J. (2001). Identification of proteins that interact with mammalian peptide:N-glycanase and implicate this hydrolase in the proteasome-dependent pathway for protein degradation. *Proc. Natl. Acad. Sci. USA* 98, 11163–11168.
 10. Suzuki, T., Park, H., Hollingsworth, N.M., Sternglanz, R., and Lennarz, W.J. (2000). PNG1, a yeast gene encoding a highly conserved peptide:N-glycanase. *J. Cell Biol.* 149, 1039–1052.
 11. Hirsch, C., Blom, D., and Ploegh, H.L. (2003). A role for N-glycanase in the cytosolic turnover of glycoproteins. *EMBO J.* 22, 1036–1046.
 12. Heemels, M.T., and Ploegh, H. (1995). Generation, translocation, and presentation of MHC class I-restricted peptides. *Annu. Rev. Biochem.* 64, 463–491.
 13. Furman, M.H., Ploegh, H.L., and Tortorella, D. (2002). Membrane-specific, host-derived factors are required for US2- and US11-mediated degradation of major histocompatibility complex class I molecules. *J. Biol. Chem.* 277, 3258–3267.
 14. Lilley, B.N., and Ploegh, H.L. (2004). A membrane protein required for dislocation of misfolded proteins from the ER. *Nature* 429, 834–840.
 15. Wiertz, E.J., Tortorella, D., Bogoy, M., Yu, J., Mothes, W., Jones, T.R., Rapoport, T.A., and Ploegh, H.L. (1996). Sec61-mediated transfer of a membrane protein from the endoplasmic reticulum to the proteasome for destruction. *Nature* 384, 432–438.
 16. Wiertz, E.J., Jones, T.R., Sun, L., Bogoy, M., Geuze, H.J., and Ploegh, H.L. (1996). The human cytomegalovirus US11 gene product dislocates MHC class I heavy chains from the endoplasmic reticulum to the cytosol. *Cell* 84, 769–779.
 17. Garcia-Calvo, M., Peterson, E.P., Leiting, B., Ruel, R., Nicholson, D.W., and Thornberry, N.A. (1998). Inhibition of human caspases by peptide-based and macromolecular inhibitors. *J. Biol. Chem.* 273, 32608–32613.
 18. Katiyar, S., Suzuki, T., Balgobin, B.J., and Lennarz, W.J. (2002). Site-directed mutagenesis study of yeast peptide:N-glycanase. Insight into the reaction mechanism of deglycosylation. *J. Biol. Chem.* 277, 12953–12959.
 19. Klausner, R.D., Lippincott-Schwartz, J., and Bonifacino, J.S. (1990). The T cell antigen receptor: insights into organelle biology. *Annu. Rev. Cell Biol.* 6, 403–431.
 20. Yu, H., Kaung, G., Kobayashi, S., and Kopito, R.R. (1997). Cytosolic degradation of T-cell receptor alpha chains by the proteasome. *J. Biol. Chem.* 272, 20800–20804.
 21. Huppa, J.B., and Ploegh, H.L. (1997). The alpha chain of the T cell antigen receptor is degraded in the cytosol. *Immunity* 7, 113–122.
 22. Powers, J.C., Asgjan, J.L., Ekici, O.D., and James, K.E. (2002). Irreversible inhibitors of serine, cysteine, and threonine proteases. *Chem. Rev.* 102, 4639–4750.
 23. Caserta, T.M., Smith, A.N., Gultice, A.D., Reedy, M.A., and Brown, T.L. (2003). Q-VD-OPh, a broad spectrum caspase inhibitor with potent antiapoptotic properties. *Apoptosis* 8, 345–352.
 24. Spiro, R.G. (2004). Role of N-linked polymannose oligosaccharides in targeting glycoproteins for endoplasmic reticulum-associated degradation. *Cell. Mol. Life Sci.* 61, 1025–1041.
 25. Suzuki, T., Park, H., Kitajima, K., and Lennarz, W.J. (1998). Peptides glycosylated in the endoplasmic reticulum of yeast are subsequently deglycosylated by a soluble peptide: N-glycanase activity. *J. Biol. Chem.* 273, 21526–21530.
 26. Weng, S., and Spiro, R.G. (1997). Demonstration of a peptide:N-glycosidase in the endoplasmic reticulum of rat liver. *Biochem. J.* 322, 655–661.
 27. Ye, Y., Shibata, Y., Yun, C., Ron, D., and Rapoport, T.A. (2004). A membrane protein complex mediates retro-translocation from the ER lumen into the cytosol. *Nature* 429, 841–847.
 28. Tortorella, D., Story, C.M., Huppa, J.B., Wiertz, E.J., Jones, T.R., Bacik, I., Bennink, J.R., Yewdell, J.W., and Ploegh, H.L. (1998). Dislocation of type I membrane proteins from the ER to the cytosol is sensitive to changes in redox potential. *J. Cell Biol.* 142, 365–376.
 29. Hochstenbach, F., David, V., Watkins, S., and Brenner, M.B. (1992). Endoplasmic reticulum resident protein of 90 kilodaltons associates with the T- and B-cell antigen receptors and major histocompatibility complex antigens during their assembly. *Proc. Natl. Acad. Sci. USA* 89, 4734–4738.
 30. Takegawa, K., Yamabe, K., Fujita, K., Tabuchi, M., Mita, M., Izu, H., Watanabe, A., Asada, Y., Sano, M., Kondo, A., et al. (1997). Cloning, sequencing, and expression of *Arthrobacter protophormiae* endo-beta-N-acetylglucosaminidase in *Escherichia coli*. *Arch. Biochem. Biophys.* 338, 22–28.
 31. Rehm, A., Stern, P., Ploegh, H.L., and Tortorella, D. (2001). Signal peptide cleavage of a type I membrane protein, HCMV US11, is dependent on its membrane anchor. *EMBO J.* 20, 1573–1582.
 32. Ponnusamy, E., Fotadar, U., Spisni, A., and Fiat, D. (1986). A novel method for the rapid, nonaqueous tert-butoxycarbonylation of some O-17-labeled amino-acids and O-17-NMR parameters of the products. *Synthesis (Stuttgart)* 7, 48–49.
 33. Palmer, J.T. May 1993. Process for forming a fluoromethyl ketone. U.S. patent 5,210,272.